

THREE-DIMENSIONAL MORPHOLOGIES OF PLANETARY NEBULAE

ARSEN R. HAJIAN

*United States Naval Observatory
Department of Astrometry* § ¶

AND

KEVIN H. KNUTH

*Center for Advanced Brain Imaging and Department of Cognitive
Neuroscience Studies, The Nathan Kline Institute* ||

Abstract.

The largest hurdle to understanding the physics of planetary nebulae is knowledge of their distances. Though measuring distances is normally a difficult problem in astronomy, measuring the distances to planetary nebulae is especially tough. The most commonly used techniques use sweeping assumptions about the population of planetary nebulae, yielding typical distance errors to these objects are usually larger than the distances themselves. To solve this problem, we have been directly measuring accurate expansion parallax distances to PNe. This technique requires dividing the Doppler expansion velocity by the angular expansion rate of the nebula, which is measured by comparing two images separated by a time baseline of a few years. The only problem with this method is that the geometry of the PN needs to be determined - otherwise it would be impossible to reliably compare the observed tangential angular motions with measured radial velocities. Therefore, we present a new method to solve for the nebular geometry with a minimum of assumptions. The model is not limited by taking into account only geometry: ionization equilibrium has been imposed in order to inject realistic physics constraints into the modeling process. Using this technique, we analyze new images of PNe obtained as part of the Expansion Parallax Project from the Hubble Space Telescope within the past two years.

§Visiting Astronomer, Kitt Peak National Observatory, National Optical Astronomy Observatories, which is operated by the Association of Universities for Research in Astronomy, Inc. (AURA) under cooperative agreement with the National Science Foundation.

¶Email: hajian@usno.navy.mil

||Email: kkunth@balrog.aecom.yu.edu

1. Introduction and Scientific Justification

The purpose of this paper is to outline a method for determining accurate distances to planetary nebulae (PNe) in our galaxy. In this section, we briefly sketch the astrophysical ingredients necessary to define the problem, and show that good distances can be derived *provided* that the three-dimensional spatiokinematic structure of the nebulae can be determined.

1.1. BACKGROUND

Stars are the result of a balance between the crushing force of gravity and the explosive force caused by the fusion of hydrogen: at some radius, the forces from these two processes cancel, enabling a star to persist at this stable radius. However, during the few million to many billion year lifetime of a stable, hydrogen-burning star, the available supply of hydrogen is depleted as it is converted into helium. At some point, the energy generated by hydrogen fusion diminishes due to a lack of fuel, and the stellar core cannot support its current dimensions due to the sudden lack of nuclear energy generation. As it collapses, the rising temperatures in the core eventually ignite helium, leading to the release of even larger amounts of nuclear energy. At this point, the star's diameter swells prodigiously, though not self-similarly, as most of the mass is concentrated in the core, which is smaller than 1% of the stellar diameter. At this point, the star is known as a red giant.

Since the stellar radius has increased due to the augmented nuclear energy generation rate in the core, the surface gravity of the star is very low. This permits material to leave the stellar surface in the form of a wind. The actual mechanics of the mass-loss process are not understood in detail, but mass-loss rates in excess of $10^{-5} M_{\odot} \text{ yr}^{-1}$ have been observed from red giant stars. As the star continues to evolve, the star appears bluer as deeper stellar layers are exposed, the mass-loss rate increases, and the character of the stellar wind changes from a thick, low-velocity neutral wind to a much faster, more tenuous ionized wind. It is currently believed that the interplay between these two winds shapes the outflow. The snow-plowing effect of the high-velocity wind compacts the thick envelope from the red giant and detaches it from the central star. The increased surface temperature of the central star yields a huge flux of ionizing photons, and the formerly neutral envelope of the star is ionized. A planetary nebula has been born.

1.2. PNE DISTANCE ESTIMATION

Traditionally, distances to astronomical objects are very difficult to determine accurately. Trigonometric parallax helps somewhat by providing perspective views of nearby objects as the earth revolves about the sun, but this is only effective for the most nearby targets. The number of PNe with trigonometric parallaxes accurate to $\lesssim 10\%$ is less than a dozen.

Statistical methods have been widely used in PN distance estimation. In general, these methods assume that some astrophysical quantity is equal to a fiducial value which is constant throughout the entire population. For example, the

most common indirect distance estimation technique is the Shklovsky method (Shklovsky 1956), which assumes that all PNe possess the same ionized mass. By virtue of the simplifying assumptions inherent to the method, the computations required to extract distance estimates are simple, can be performed with a simple calculator or spreadsheet, and are thus conducive to large samples of targets. Although conclusions gleaned from such studies have implications for the entire PN population in a statistical sense, distances to individual PNe with this method are not meaningful. For example, the masses of the progenitor stars to PNe range from 0.8-8 M_{\odot} , and the assumption of a constant ionized mass introduces an error of $\approx 150\%$ to the distance.

The situation with PNe distances is therefore grim: a substantial fraction of PNe in our galaxy have distances that are less accurately known than distances to PNe in other galaxies.

Knowledge of the distance scale is crucial for estimating the astrophysical parameters of PNe, which in turn have significant implications for the generation and maintenance of various galactic quantities. Until the distance scale to PNe is established, the physical quantities pertaining to the central star and nebula will be hard to constrain (such as mass, luminosity, radius, etc.), and this makes comparison with evolutionary theories difficult to perform. In addition, the amount of material being reintroduced into the interstellar medium (Pottasch 1984) and the white dwarf birthrate and subsequent maintenance of part of the ionizing flux of the galaxy (Panagia & Terzian 1984; Terzian 1974) are also strongly distance-dependent. Finally, studies of galactic rotation involving PNe (Schneider & Terzian 1983) have been limited due to the uncertainty in the distance to the PNe used to trace the galactic potential.

In an effort to solve this problem, we have been measuring expansion parallax distances to PNe (Hajian, Terzian, & Bignell 1993, 1995). This technique requires dividing the Doppler expansion velocity by the angular expansion rate of the nebula, which is measured by comparing two images separated by a time baseline of a few years. The only problem with this method is the geometry of the PN, which is required in order to marry angular (tangential) expansions with radial velocities. Imprecise knowledge of the nebular geometry can cause systematic distance errors much larger than the stochastic errors (which can be as small as 10%).

So far, the expansion parallax method has been applied to a small sample of PNe. Nevertheless, the initial results are very promising. To date, roughly half of the dozen objects observed with the Very Large Array in Socorro, NM, have yielded accurate expansion parallax distances. In addition, all four of the targets we have investigated with two epochs of HST data have shown obvious expansion signatures.

2. Ionization-bounded Geometries

2.1. THE MODEL

Our goal is to deduce the three-dimensional structure of PNe using an image and a discrete set of longslit spectra at several slit positions.

For the most part, the shells of PNe are acceptably approximated by projected, prolate, ellipsoidal shells. We adopt this formalism, which is known as the Prolate Ellipsoidal Shell (PES) model (Aaquist & Kwok 1990; Masson 1989; Zhang & Kwok 1998), and sketch our implementation of the classical model below.

We begin with a central star which is a source of ionizing photons. This star is surrounded by a hydrogen density distribution, $n(\theta, \phi, r)$. We treat this situation similar to that of a Stromgren sphere: the star ionizes the gas to a radius $R_o(\theta, \phi)$ depending on the intervening column density of hydrogen gas (*i.e.*, the nebula is ionization bounded). In addition, we assume the inner cavity of the PN out to a distance $R_i(\theta, \phi)$ has been vacated by the high-velocity wind from the central star. If we equate the number of ionizing photons along a line-of-sight (left-hand side below) to the number of local recombinations (right-hand side below), we arrive at:

$$L = \int_{R_i}^{R_o} \int_0^{2\pi} \int_0^\pi \alpha_B n^2(\theta, \phi, r) r^2 dr \sin(\theta) d\theta d\phi, \quad (1)$$

where L is the stellar ionizing luminosity and α_B is the hydrogen recombination coefficient (excluding captures to the ground state). We can write this as:

$$\frac{dL}{d\Omega} = \int_{R_i}^{R_o} \alpha_B n^2(\theta, \phi, r) r^2 dr. \quad (2)$$

Now we define the density distribution, $n(\theta, \phi, r)$, by separating it into three components:

$$n(\theta, \phi, r) = n_o \eta_\theta(\theta) \eta_\phi(\phi) \eta_r(r), \quad (3)$$

where $n_o = n(0, 0, R_i)$, the angle θ is measured with respect to the polar axis of the nebula, and the angle ϕ with respect to the North (on the sky). Note that the model PN is symmetric with respect to the angle θ . If we choose a radial power law distribution of the form:

$$\eta_r = \left(\frac{r}{R_i} \right)^{-\gamma}, \quad (4)$$

then equation (2) has an analytic solution of the form:

$$\frac{dL}{d\Omega} = \frac{\alpha_B n_o^2 \eta_\theta^2 \eta_\phi^2 R_i^3}{-2\gamma + 3} \left[\left(\frac{R_o}{R_i} \right)^{-2\gamma+3} - 1 \right] \quad (5)$$

The above model is physically meaningful only if $\frac{dL}{d\Omega} > 0$ and if $R_i < R_o$, which can only be satisfied for $\gamma < 1.5$. The azimuthal density distribution is parametrized with the constants α and β :

$$\eta_\theta = \{(1 - \beta) \left[\left(\frac{2\theta}{\pi} \right)^\alpha + \frac{\beta}{1 - \beta} \right]\}, \quad \text{for } 0 \leq \theta \leq \frac{\pi}{2} \quad (6)$$

$$= (1 - \beta) \left[\left(\frac{2\pi - 2\theta}{\pi} \right)^\alpha + \frac{\beta}{1 - \beta} \right], \quad \text{for } \frac{\pi}{2} \leq \theta \leq \pi. \quad (7)$$

For the kinematic portion of the model, we assumed that since all of the nebular gas was present at the location of the central star at some point in time, that the

expansion velocity of the gas is purely radial and that the magnitude of the velocity is proportional to the distance from the central star.

2.2. IMPLEMENTATION

We implemented the model described above as follows. First, we begin with an ellipsoidal surface, R_i , in the frame of the PN defined by two parameters: the length of the major axis, $R_{i,\text{major}}$, and the axial ratio, ϵ . The third parameter is the ionization parameter, ξ :

$$\xi = \frac{\left(\frac{dL}{d\Omega}\right)}{(n_o \eta_\phi)^2 \alpha_B} \quad (8)$$

and was used in conjunction with α , β , and γ to describe the density distribution, and then to compute $R_o(\theta, \phi)$. The intensity at each voxel is set equal to $\alpha_B n^2$ provided the voxel is between $R_i(\theta, \phi)$ and $R_o(\theta, \phi)$.

The three-dimensional structure of the PN is then rotated into the observer's frame using the angles i and θ' , which are the inclination relative to the line of sight and the position angle on the sky relative to N, respectively. The intensities are integrated along the line-of-sight to form a two-dimensional model representing the brightness of the PN on the sky.

Kinematic modelling requires the addition of a single parameter: the equatorial velocity, $v_o = v(0, 0, R_i)$. The velocity in each voxel is oriented away from the central star and the magnitude is proportional to the distance from the central star (normalized to v_o). After rotating the PN to the desired orientation, model longslit spectra can be synthesized for each image pixel by integrating the intensity-weighted radial velocity for each voxel in the line-of-sight.

In summary, our image model is defined by ξ , α , β , γ , $R_{i,\text{major}}$, ϵ , i , and θ . The kinematic model requires v_o in addition.

Once the model is defined, we invoke Bayes Theorem:

$$P(\text{model}|\text{data}, I) = P(\text{model}|I) \frac{P(\text{data}|\text{model}, I)}{P(\text{data}|I)}. \quad (9)$$

Since the image, $X_{i,j}$, and kinematic data, $Y_{m,n}$, are independent of one another, we can write:

$$P(\text{model}|X, Y, I) = P(\text{model}|I) \frac{P(X|\text{model}, I)P(Y|\text{model}, I)}{P(X, Y|I)}. \quad (10)$$

In our initial attempts at solving this problem, we have adopted Gaussian likelihood functions, $P(X|\text{model}, I)$ and $P(Y|\text{model}, I)$, and uniform priors, $P(\text{model}|I)$.

3. Results to Date

On the observational side, we have been engaged in an observing program of a sample of PNe: images have been obtained using the Hubble Space Telescope (HST) and longslit spectra with the Kitt Peak (KPNO) and the Cerro-Tololo (CTIO) 4-m Echelle Spectrographs. Our criteria for selecting PNe for observation

was their potential for yielding measurable expansion parallaxes. The factors we deemed most necessary were:

- 1) *Regular and Simple Appearance*: The morphology of the nebula based on ground-based images must be regular and elliptical. Irregular nebula were to be generally avoided.
- 2) *Smooth Surface*: The nebular structure must be smooth and should not be significantly contaminated by knots, jets, globules, or any other microstructure, since these compact structures may have anomalous velocities (and that are difficult to deproject), and so do not share in the bulk flow of the nebular gas.
- 3) *Sharp Edges*: Edges of large-scale structures such as rims should be sharp (*i.e.*, large radial flux gradient).
- 4) *Bright Lines*: The nebula is required to be bright in the lines of $[\text{N II}]\lambda 6584\text{\AA}$ and $[\text{O III}]\lambda\lambda 5007\text{\AA}$.
- 5) *Large Expansion Velocity*: Some preference was given to PNe with large equatorial expansion velocities.
- 6) *Nearby*: Although statistical distances are suspect for individual PNe, some preference was given to PNe that are statistically nearby.

Among the plethora of applicants, we selected 30 PNe which satisfied the above constraints, and observed them using the Wide Field Planetary Camera 2 onboard the HST through the F658N, F502N, and F555W filters. The first two of these were narrowband filters used to isolate the $[\text{O III}]\lambda\lambda 5007\text{\AA}$ lines and the $[\text{N II}]\lambda 6584\text{\AA}$ line, and the last filter corresponds to the broadband V filter. As of the date of this manuscript, 14 of these PNe have one epoch of data and 10 have two. Examples of the imaging data from the HST are shown in Figure 1. With angular resolutions of a few tens of milliarcseconds, the images from HST are approximately 20 times more resolved than groundbased images from conventional telescopes, which are limited to $\approx 1''$ resolution due to the imaging limitations imposed by atmospheric turbulence.

In addition, longslit spectroscopy observing runs were obtained at the KPNO in June 1999 (4 nights) and April 2000 (2 nights) and at CTIO in May 1999 (4 nights) and June 2000 (4 nights). All 30 of the HST targets have been observed at KPNO or CTIO in addition to 25 targets for which we will secure future imaging observations. An example of the longslit observational data from NGC 6741 is shown in Figure 2.

Figure 3 shows our initial attempts to model the V band image of IC 418. The model we have derived is not the best fit, but merely a good fit that results from an absolutely impossible initial guess and several iterations of a simple grid Monte Carlo search performed one variable at a time. We are currently in the process of implementing an annealing algorithm to perform a Markov chain Monte Carlo search for the optimum model. Burn-in will be accomplished using the prior probability distribution, and then more and more of the likelihood function will be allowed to contribute to the posterior. The total posterior will likely be sharply peaked near the best solution: ambiguous situations, such as a round PN versus a elliptical PN being viewed pole-on, will be unambiguously resolved with the inclusion of the longslit spectra.

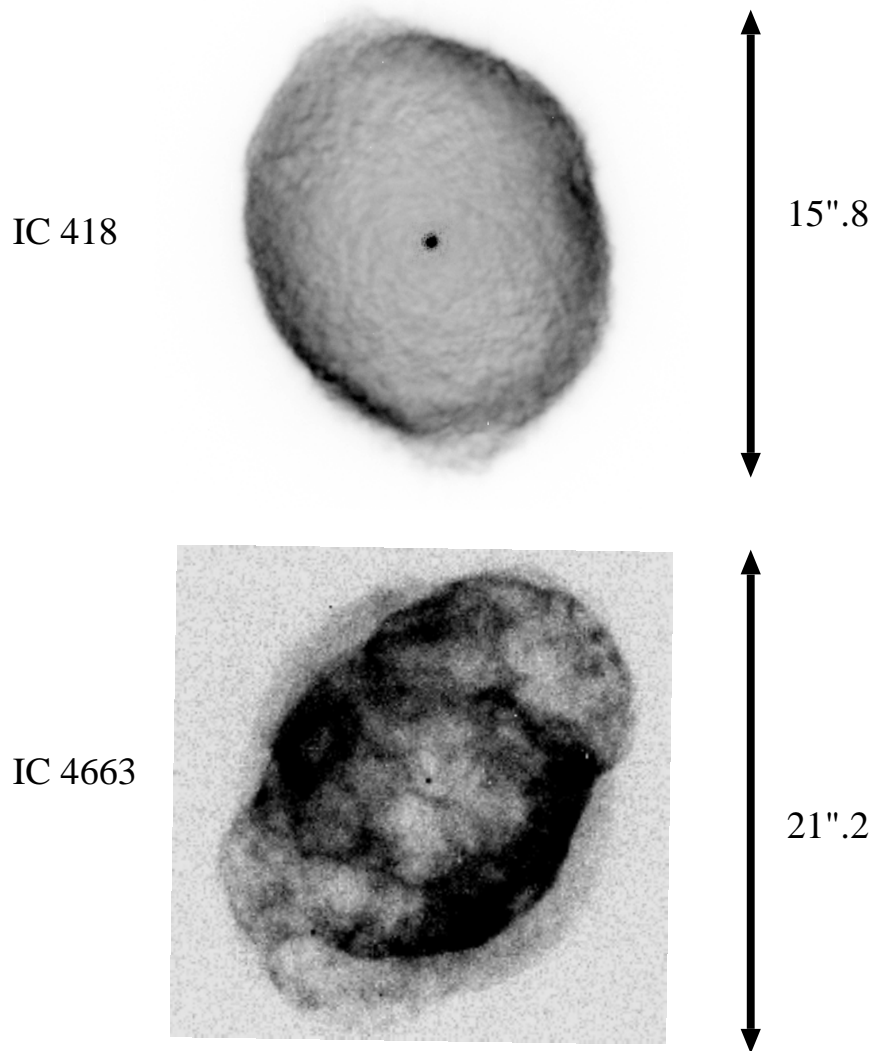


Figure 1. This figure shows calibrated HST images IC 418 in the light of [N II] (top) and IC 4663 in the light of [O III] (bottom).

One complicating factor is the duration of the calculation: on a 500 MHz pentium, our C implementation of the above algorithms requires ≈ 10 seconds to generate a 200x200 pixel model image and six 200x50 pixel longslit spectra. Since the annealing procedure requires the generation of roughly 10^4 such images, we expect it to take approximately one day to determine the best-fit model per PN. Efforts

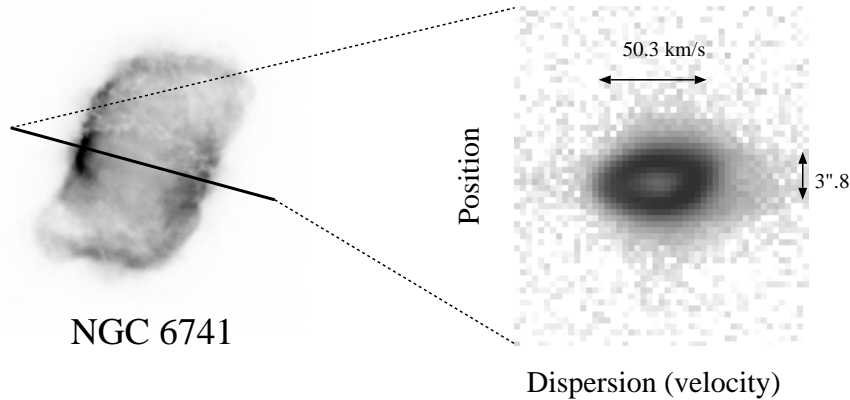


Figure 2. This figure shows the calibrated image and longslit spectrum of the PN NGC 6741 observed in the light of [O III]. The slit position is shown in the image going through the nebular minor axis. The expansion of the PN has been resolved, and appears to be approximately 25 km s^{-1} .

are underway to reduce this time.

4. Acknowledgements

The authors would like to thank Larry Bretthorst for several insightful discussions. A.H. would like to thank his collaborators on the Expansion Parallax Project: Bruce Balick, Howard Bond, Stefano Casertano, Stefano Giovanardi, Tracy Klayton, Steve Movit, Stacy Palen, Nino Panagia, Darren Reed, Yervant Terzian. This work was supported by NASA through grants GO-7501, GO-8390, and GO-8773 from the Space Telescope Science Institute, which is operated by the Associated Universities for Research in Astronomy, Inc., under NASA contract NAS5-26555.

References

- Aaquist, O.B., & Kwok, S. 1990, A&AS, 84, 229.
- Hajian, A.R., Terzian, Y., & Bignell, C. 1993, AJ, 106, 1965.
- Hajian, A.R., Terzian, Y., & Bignell, C. 1995, AJ, 109, 2600.
- Masson, C.R. 1989, ApJ, 346, 243.
- Panagia, N., & Terzian, Y. 1984, ApJ, 287, 315.
- Pottasch, S. *Planetary Nebulae*, 1984, (Reidel:Dordrecht), p. 274.
- Schneider, S.E., & Terzian, Y. 1983, ApJ Lett., 274, L61.
- Shklovsky, I.S. 1956, AZh, 33, 222.
- Terzian, Y. 1974, ApJ, 193, 93.
- Zhang, C.Y., & Kwok, S. 1998, ApJS, 117, 341.

IC 418

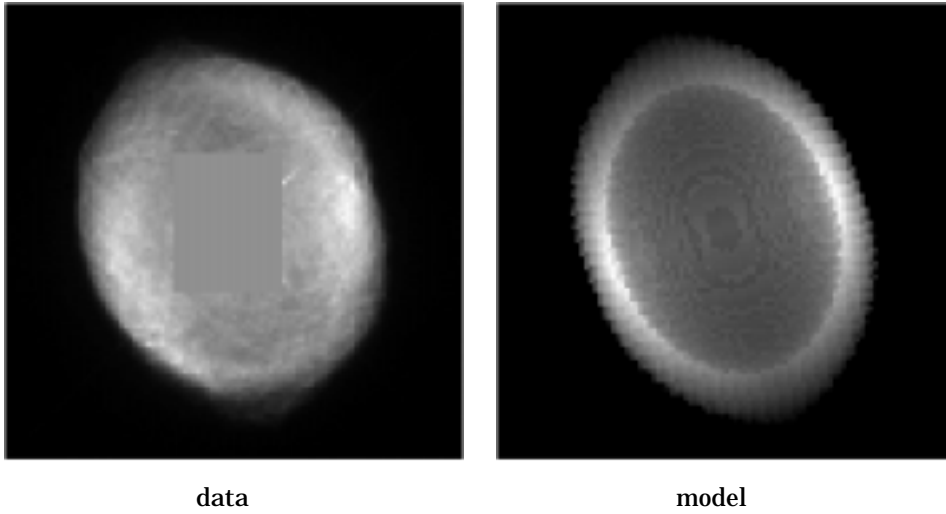


Figure 3. This figure shows the intermediate results from fitting a model of an ionization bounded prolate ellipsoid (right) to the image of IC 418 observed through the broadband V filter (left). We have masked the central star and associated diffraction spikes in the HST image of IC 418 with a uniform intensity patch to avoid biasing the nebular fit.